

NEDLA TEST SITE REPORT

Amur Site

Tatiana Loboda ¹, Guoqing Sun ^{1,2}, Zhiyu Zhang ¹

¹University of Maryland, Geography Department

²NASA Goddard Space Flight Center

Contents

1	Site Location	3
1.1	Country, State, Province	3
1.2	Center coordinates	3
1.3	Geographic settings and environmental characteristics	3
1.4	Land Use	4
1.5	Major types of vegetation disturbance and land cover change	4
2	Satellite Imagery	4
3	Auxiliary data	4
4	Mapping Legend	5
5	Land Cover Map	7
5.1	Pre-processing	7
5.2	Land cover classification	8
5.2.1	Masks	8
5.2.2	Development of metrics for image classification	9
5.2.3	Mapping vegetation classes	9
5.3	Post-classification processing	9
5.4	Accuracy assessment	9
5.4.1	Aggregated classes accuracy assessment	9
5.4.2	Full classification accuracy assessment	10
5.5	Analysis of mapping results	12
5.6	Comparison to coarse resolution land cover maps	13
6	Land Cover Change Map	15
6.1	Pre-processing	15
6.1.1	Mature forest mapping	15
6.1.2	Accuracy assessment for mature forest mapping	15
6.1.2.1	Scene from June 15, 1987	15
6.1.2.2	Scene from July 5, 2006	16
6.2	Change detection	16
6.3	Post-classification processing	17
6.4	Accuracy assessment	17
6.5	Results of the land cover change map	18
6.6	Analysis of the land cover change map	20
7	Publications Using the Site Data	22

8	List of Contributors to Site Data and Report	22
9	Acknowledgements	22
10	References	22

1 Site Location

1.1 Country, State, Province

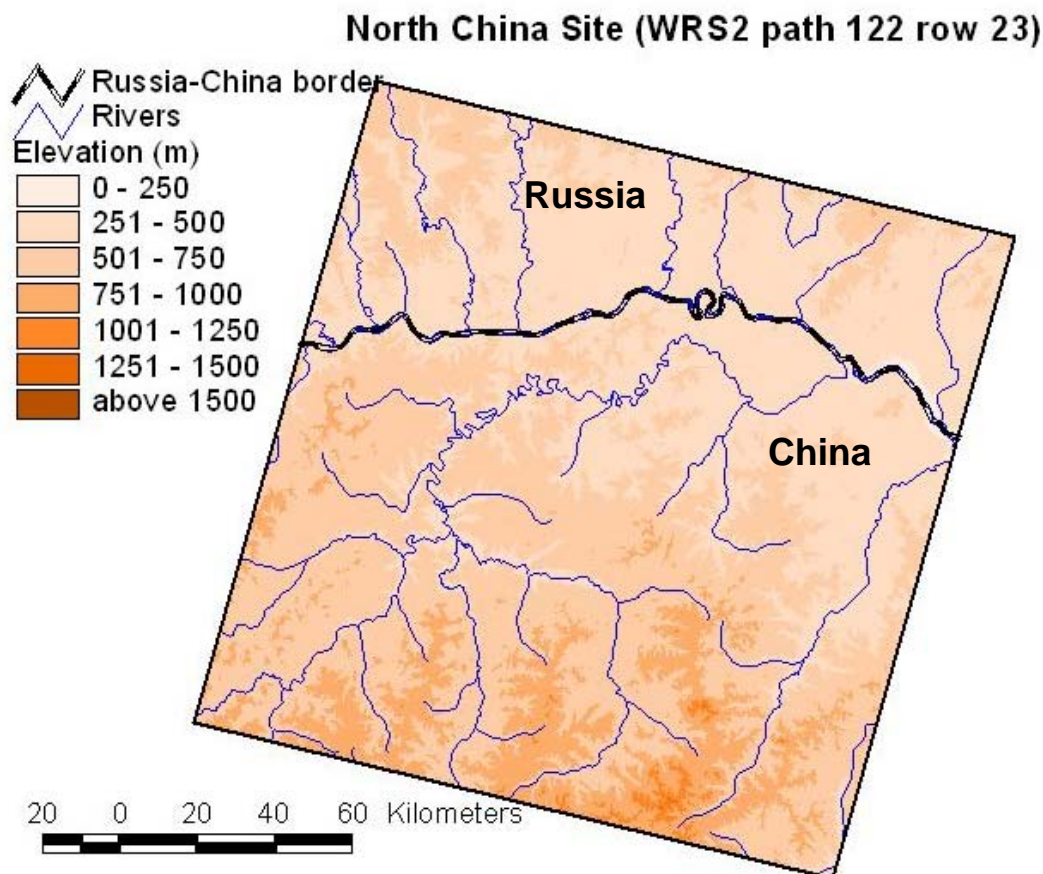
The test site is located on the border between the Amur Oblast of the Russian Federation and the north west of the Heilongjiang Province of the People's Republic of China.

1.2 Center coordinates

53.1° N, 123.1° E (Landsat WRS2 path 122 row 23)

1.3 Geographic settings and environmental characteristics

The site is located in southern taiga of Eastern Siberia and Northern China. The site spans across the Amur river stretching between the Amur Oblast in the north and Daxinganling Prefecture, including the Hulun Buir Grassland along the Amur river and the Songnen Plain in the eastern part of the site, in the south. The elevation ranges between 200 and 1400 m above sea level with the mean elevation around 600m.



The region's ecosystems developed in cold climatic conditions with mean annual temperatures ranging between -5°C in the north to 4°C in the south and are characterized by large inter-annual

variability. The intra-annual variability in temperatures is also very large (~ 40°C) and is explained by the extremely continental climate of the study site (Stolbovoi and McCallum, 2002). The climate is characterized by long cold winters and short hot summers with roughly 100-180 frost-free days per year. The site receives 200-400 mm of rainfall annually but has high levels of evapotranspiration (600-800 mm annually) subsequently resulting in moisture deficit conditions and presence of dwarf-shrubs and ephemeroids. The site has a considerable above and below ground living biomass density with the net primary production of carbon around 0.21-0.28 kg/m²/y (Stolbovoi and McCallum, 2002). The forests are mainly distributed over the mountains. Cold-temperate needle-leaf forests, dominated by *Larix gmelii* are distributed in the north part of Daxinganling (the Greater Xing'an Mountains), while the deciduous broad-leaf forests of the temperate zone, dominated by *Quercus mongolica*, *Populus davidiana*, and *Betula platyphylla*, are distributed in the middle and southern parts of Daxinganling.

1.4 Land Use

The majority of the area is within commercial forestry use with small sections used for crop production and rangelands. This area is one of the most important timber production sites in China and is also zoned for timber harvesting within Russia.

1.5 Major types of vegetation disturbance and land cover change

Timber harvesting presents the major type of anthropogenic disturbance on both side of the border. Natural disturbances are represented by wildland fire and insect infestation. An extremely large fire occurred on the Chinese side of the site in 1987 with smaller scars found in other areas of the image. While the forests on the Russian side recovered from 1987 fire naturally and experienced new fires (such as in 1998 and in 2003), the Chinese government implemented a 10-year program to suppress forest fire and plant trees in the burnt area. Chinese government has implemented a new forest policy, the Natural Forest Conservation Program (NFCP) (Zhang et al., 2000; Zhao and Shao, 2002), since 1999 but logging is still continuing in smaller scale. The pine forests of the area are also susceptible to nun moth infestations with the infestation probability between 25 and 50 % (Stolbovoi and McCallum, 2002).

2 Satellite Imagery

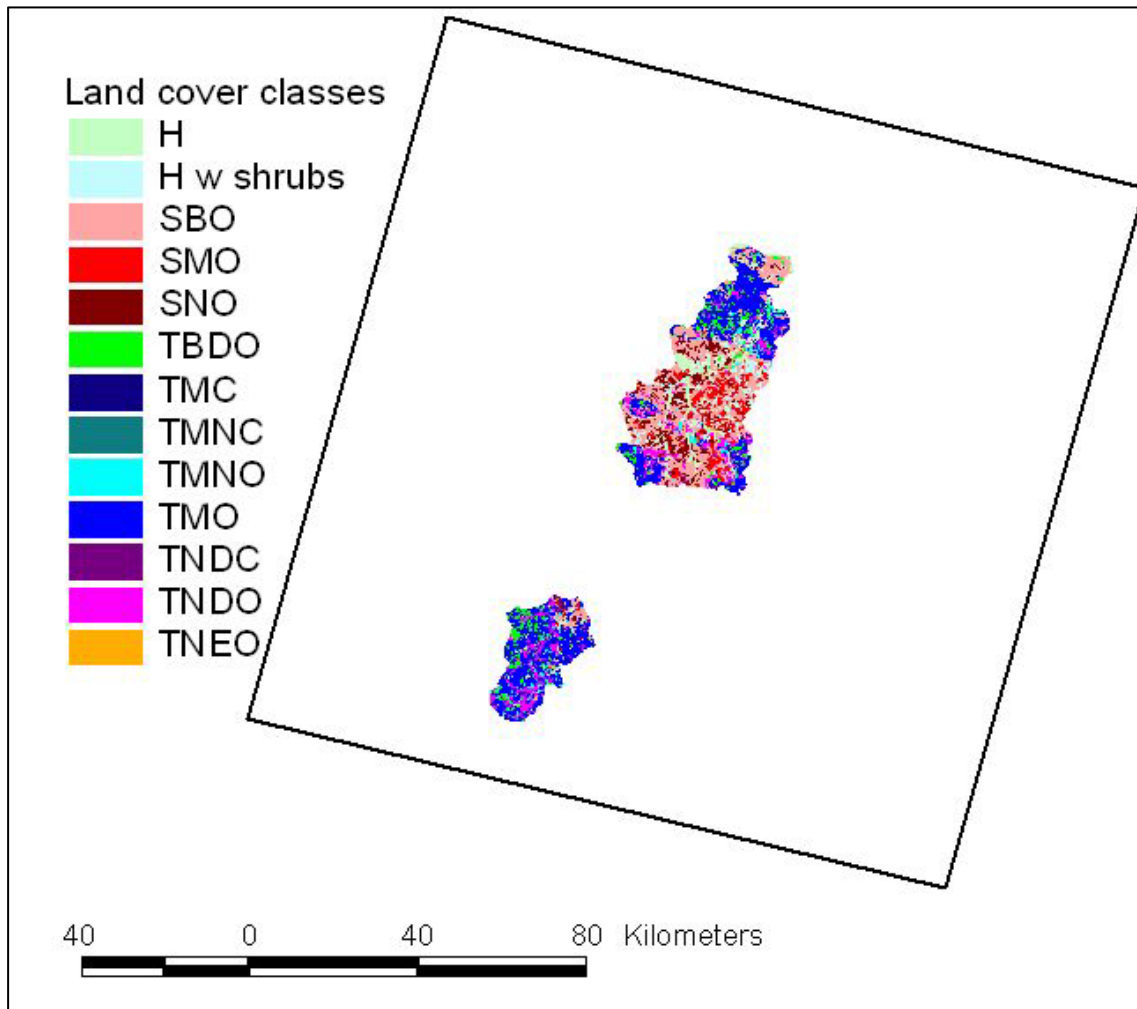
Landsat MSS (WRS1 p132 r 23), TM, and ETM+ (WRS2 p 122 r 23) images present the primary source of data for land cover mapping and change detection. The image stack includes 7 images and covers the time period between 1974 and 2006.

Instrument	Acquisition date	Use	Notes
Landsat MSS	01/13/1974	secondary	reference winter scene
Landsat TM	06/12/1986	secondary	pre-burn scene for 1986 fire
Landsat TM	06/15/1987	primary	change detection basis, post-burn scene
Landsat TM	08/11/1999	secondary	post-fire vegetation regrowth
Landsat ETM+	09/14/2000	secondary	post-fire vegetation regrowth
Landsat ETM+	05/15/2002	primary	classification basis, change detection basis
Landsat TM	07/05/2006	primary	change detection basis

3 Auxiliary data

QuickBird images available at GoogleEarth were visually examined to identify sites for urban areas and cultivated lands as well as in defining training and validation pixels for the classification. In addition, the Shuttle Radar Topography Missions (SRTM) dataset was used to apply topographic correction to image data values.

In situ forest inventory polygons collected during the year 2000 and covering ~ 6 % of the Landsat scene were included as a reference and validation data set for accuracy assessment of mature forest mapping within the change detection component of the analysis (see section 6).









The inventory data were converted to the NELDA land cover classes using the auxiliary information regarding species composition, age, height, and canopy closure of the surveyed stands. Although forest inventory data contains detailed spatially explicit information regarding land covers within the test site, previous experience showed that its resolution is insufficient for using it as training or “per-pixels validation” datasets. Therefore, these data were only used as a reference and for relative accuracy assessment for change detection datasets.

4 Mapping Legend

The following land cover classes consistent with the NELDA Land Cover Legend were identified within the scene.

<i>Class ID</i>	<i>Description</i>	<i>Examples</i>
1	Tree.needleleaf.deciduous.closed	
2	Tree.needleleaf.deciduous.open	
3	Tree.mixed.closed	
4	Tree.mixed.open	
5	Tree.broadleaf.deciduous.closed	
6	Tree.broadleaf.deciduous.open	
7	Tree.mixed.open.mortality	
8	Tree.mixed.open.built	

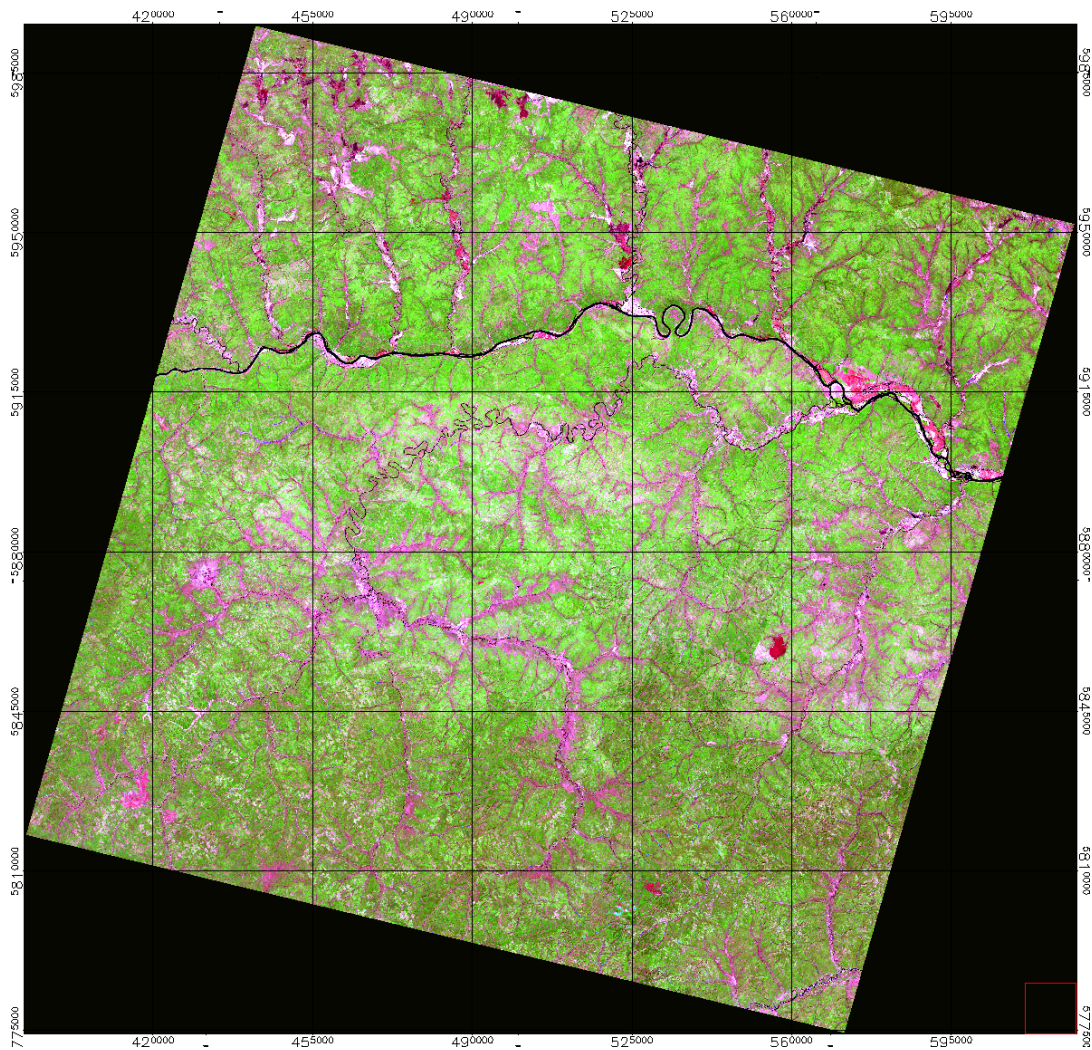
9	Shrub.mixed.closed	
10	Shrub.mixed.open	
11	Herbaceous	
12	Bare.sparse	
13	Bare.built	
14	Water	

5 Land Cover Map

5.1 Pre-processing

The main classification image was orthorectified as part of the Tri-decadal Landsat Orthorectified archive (http://eros.usgs.gov/products/satellite/landsat_ortho.php). Further image pre-processing involved performing terrain correction using the SRTM DEM data obtained from the Global Land Cover Facility (<http://glcf.umiacs.umd.edu/index.shtml>) following the methodology for the sun-canopy-sensor topographic correction in forested terrain (Soenen et al., 2005). The topographic correction was performed on the digital numbers which were subsequently converted to at sensor reflectance and atmospherically corrected using the COST method (Chavez, 1996).

Landsat/ETM+ image from 05/15/2002



5.2 Land cover classification

5.2.1 Masks

Several masks were developed prior to classifying the image to eliminate potential confusion of classes:

- i) background mask – areas of the image which contain no valid data values
- ii) water mask – thresholded in NIR and hand digitized
- iii) fresh burns were mapped using supervised Spectral Angle Mapping approach and MODIS active fire detections (see specific description of the approach in Loboda et al., 2007)
- iv) “built up” mask was developed from the GIS shapefiles of human settlements

5.2.2 Development of metrics for image classification

Additional metrics were calculated to support decision tree application:

- i) Normalized Burn Ratio (NBR)
- ii) NDVI
- iii) Principal Components
- iv) Tasseled Cap (using surface reflectance indices published in Crist, 1985)

These metrics and the original 7 bands (including resampled thermal band) were stacked in one file.

5.2.3 Mapping vegetation classes

- i) Training samples for visually identifiable in high resolution (Quickbird available at Google Earth) and the classification image from 5/15/2002 were selected across the classification scene.
- ii) Training spectra for each class from the full stack of classification metrics were extracted and reformatted for further processing in the statistical software
- iii) S-Plus statistical package was used to develop a decision tree algorithm
- iv) the decision tree rules were implemented within the “vegetative cover” mask developed after exclusion of background, water, and fresh burns.

5.3 Post-classification processing

Classes within the “built up” mask were divided into “tree.built” and “bare.built” classes after the decision tree classification. The developed classes from all steps of classification were combined into a single classification scheme according to legend presented in section 4. The resultant land cover map was sieved following the “ ≥ 5 contiguous pixels” rule to eliminate speckle. The filtered pixels were assigned a max value from a 3X3 matrix.

5.4 Accuracy assessment

Accuracy assessment was conducted following the accuracy assessment protocol developed by Dr. Krankina. It presents a combination of in situ data and randomly distributed additional points in classes that are poorly represented by ground data. The distribution of the accuracy assessment points overall proportional to the areal distribution of the mapped classes and consists of minimum of 300 randomly selected points across the image. For classes, where the proportional representation of 300 total points results in a sample of fewer than 30 points, additional random points are added to a minimum of 30 points in a sample class. According to the protocol two types of accuracy assessment are presented: 1) an assessment for 5 aggregated land cover classes including trees, shrubs, herbaceous cover, barren lands, and water; and 2) an assessment for the full set of classes identified within the site.

5.4.1 Aggregated classes accuracy assessment

For the accuracy assessment of the aggregated classes random points across the full extent of the classification were selected proportionally to the area of the class but no less than 30 pixels per class (see section 5.4). These random points were further assigned by the analyst to one of the 5

aggregated classes based on the surface reflectance characteristics and high resolution QuickBird images available at Google Earth.

		Observed Class					Sum	Commission
		Trees	Shrubs	Herbaceous	Barren	Water		
Predicted Class	Trees	277	25	0	0	0	302	8.28
	Shrubs	13	66	1	1	0	81	18.52
	Herbaceous	0	8	41	6	0	55	25.45
	Barren	0	1	14	54	0	69	21.74
	Water	1	0	0	0	35	36	2.78
	Sum	291	100	56	61	35	543	
Omission		4.81	34	26.79	11.48	0		
Overall Accuracy =87.1087 %								
Kappa Coefficient = 0.8003								

5.4.2 Full classification accuracy assessment

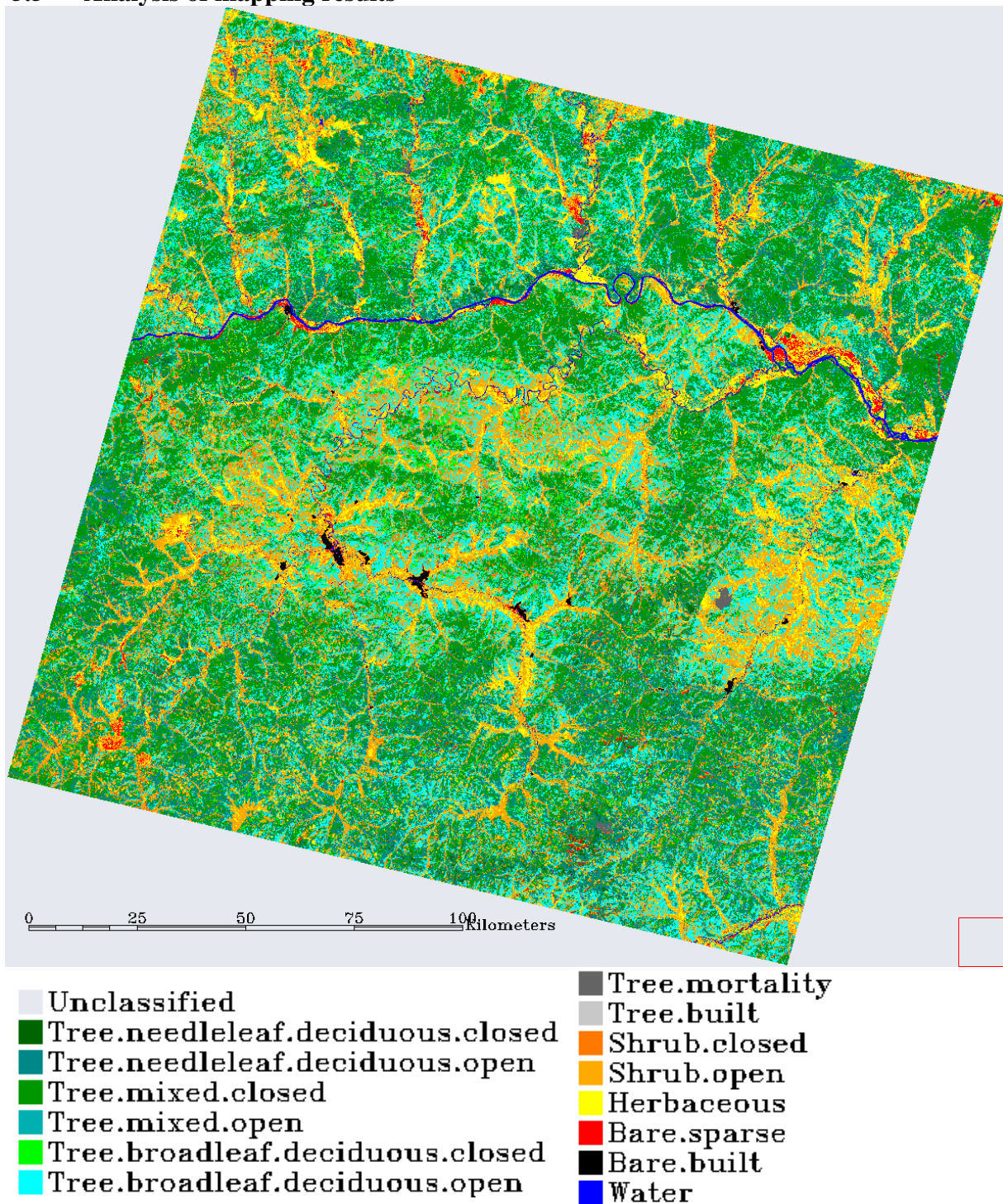
For the accuracy assessment of the full classification “Tree.mortality” and “Tree.built” classes were removed because they did not have a representative sample within the high resolution validation data. Selection of random points for the validation was limited to the extent of the available QuickBird imagery in Google Earth to ensure the ability to differentiate between classes. Random points which were not confidently identified by the analyst were removed from further validation and replaced with a new set of points.

Predicted Class	Observed Class												Sum	Commission (%)
	TNDC	TNDO	TMC	TMO	TBDC	TBDO	SC	SO	H	BS	BB	W		
TNDC	28	1	2	1	0	0	0	0	0	0	0	0	32	12.5
TNDO	2	38	3	4	0	0	0	0	0	0	0	0	47	19.15
TMC	0	0	80	11	8	0	0	1	0	0	0	0	100	20
TMO	0	1	0	6	0	0	0	1	0	0	0	0	8	25
TBDC	0	0	0	0	23	4	2	0	0	0	0	0	29	20.69
TBDO	0	0	3	10	6	46	1	20	0	0	0	0	86	46.51
SC	0	0	0	0	2	2	20	2	0	1	0	0	27	25.93
SO	0	0	0	2	0	7	1	43	1	0	0	0	54	20.37
H	0	0	0	0	0	0	0	8	41	4	2	0	55	25.45
BS	0	0	0	0	0	0	0	1	6	26	1	0	34	23.53
BB	0	0	0	0	0	0	0	0	8	0	27	0	35	22.86
W	0	0	1	0	0	0	0	0	0	0	0	35	36	2.78
Sum	30	40	89	34	39	59	24	76	56	31	30	35	543	
Omission (%)	6.67	5	10.11	82.35	41.03	22.03	16.67	43.42	26.79	16.13	10	0		

Overall Accuracy = 76.06%

Kappa Coefficient = 0.7341

5.5 Analysis of mapping results



The results of the Landsat/ETM+ classification were analyzed as percent of cover within the full extent of the Landsat scene (path 122 row 23). According to the classified image, closed mixed tree stands dominate the land cover of the Amur site (~30%). Overall tree dominated land cover

accounts for ~70% of the total area with the remaining area covered by shrubs (21%), herbaceous (7%), bare and sparse (1%) vegetation, and water (1%). Small human settlements are distributed along major rivers with bare.built category accounting for 0.2% of the total scene.

Distribution of land cover classes

<i>Class</i>	<i>Pixel</i>	<i>Area (ha)</i>	<i>% of site</i>
Tree.needleleaf.deciduous.closed	405422	32,920	0.97
Tree.needleleaf.deciduous.open	5608049	455,374	13.40
Tree.mixed.closed	12368552	1,004,326	29.55
Tree.mixed.open	449566	36,505	1.07
Tree.broadleaf.deciduous.closed	1493915	121,306	3.57
Tree.broadleaf.deciduous.open	8767660	711,934	20.95
Tree.mortality	44201	3,589	0.11
Tree.built	3236	263	0.01
Shrub.closed	1683128	136,670	4.02
Shrub.open	7178507	582,895	17.15
Herbaceous	2945852	239,203	7.04
Bare.sparse	436288	35,427	1.04
Bare.built	70714	5,742	0.17
Water	393897	31,984	0.94

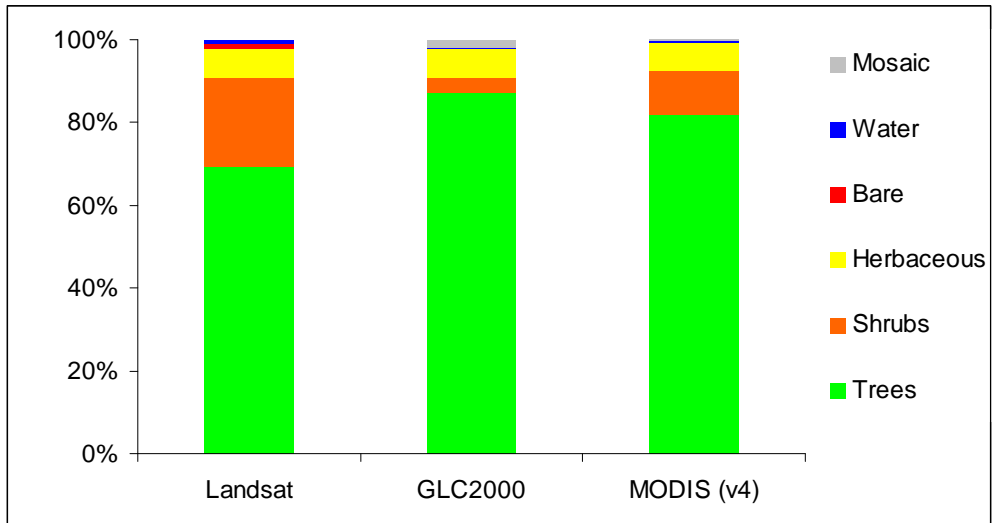
5.6 Comparison to coarse resolution land cover maps

The Landsat-based classification results were compared to the several coarse resolution products. Individual classes within each of the products were aggregated to general groups: tree dominated, shrub dominated, herbaceous dominated, bare, water and mosaic/other. IGBP-based classification was used for coarse resolution products. During the aggregation procedure cropland class was mapped as “herbaceous dominated”.

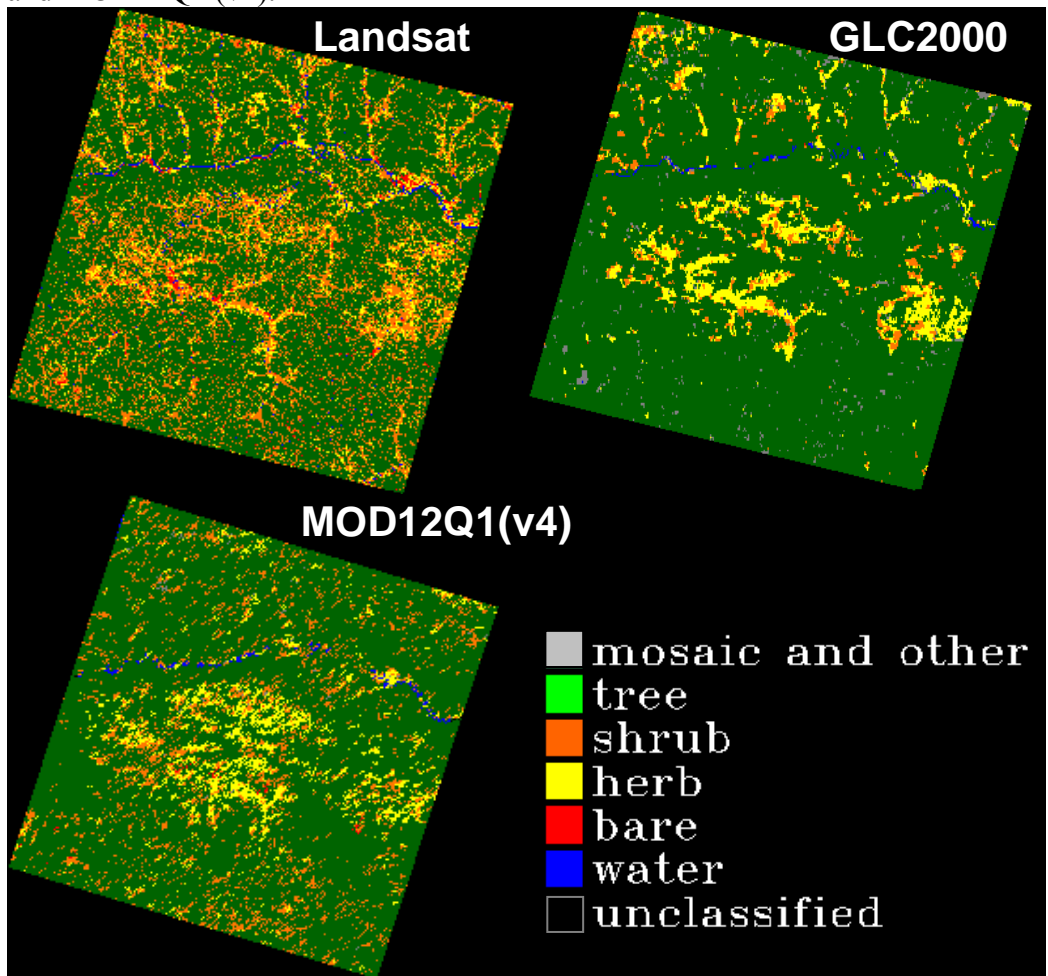
Distribution of aggregated land cover types in the Landsat, GLC2000, and MODIS (MOD12Q1) land cover products (percent):

<i>Class</i>	<i>Landsat</i>	<i>GLC2000</i>	<i>MODIS (v4)</i>
Tree dominated	69.631	86.939	82.092
Shrub dominated	21.175	3.865	10.472
Herbaceous dominated	7.039	7.063	6.660
Bare	1.212	0.004	0.114
Water	0.941	0.332	0.452
Mosaic and other	N/A	1.789	0.210

Percent land cover within the extent of the Landsat scene (path 122 row 23) mapped by the ETM+, GLC2000, and MOD12Q1 (v4).



Spatial variations in distribution of aggregated land cover types mapped by ETM+, GLC2000, and MOD12Q1 (v4).



6 Land Cover Change Map

6.1 Pre-processing

Three Landsat TM and ETM+ scenes for the study site were selected to use in change detection mapping: a) June 15, 1987, b) May 15, 2002; c) July 5, 2006 (see section 2). Each of the scenes was visually examined to determine its acquisition during the “leaf on” season and had minimal cloud cover. The scenes were geometrically co-registered to the scene from May 15, 2002 with $RMS < 0.5$. The scenes were converted to surface reflectance with correction of reflectance values according to variation in sun illumination angles due to topographic features using the methodology described in section 5.1.

6.1.1 Mature forest mapping

Water, shadow, cloud, and “mature forest” (defined by the analyst) were identified in the imagery. First, shadow, clouds, and water masks were created using band thresholding and subsequent analyst-driven selection. Second, multivariable stacks including surface reflectance for bands 1-5 and 7, NDVI, NBR, and Tasseled Cap (TC) transforms (using surface reflectance coefficients (Crist, 1985)) for brightness, greenness, and wetness parameters were compiled for each scene. Third, maximum likelihood classification for four classes, including 1) bare and sparsely vegetated, 2) shrub dominated, 3) tree dominated, and 4) tree dominated with mortality classes with a 0.7 probability threshold was run on the 1987 and 2006 scenes masking out classes identified in step 1. Mature forests for 2002 image were identified based on the detailed classification including all tree dominated classes with the exception of “tree dominated with mortality” class.

6.1.2 Accuracy assessment for mature forest mapping

The results of the maximum likelihood classifications for mature forests within scenes from 1987 and 2006 were compared to in situ forestry inventory data collected in year 2000. Considering the time difference between the acquisition of inventory data and the classified images only mature forest accuracy was assessed.

6.1.2.1 Scene from June 15, 1987

In situ forest inventory digital polygons for tree dominated communities were binned into 5-year categories beginning with stand age 20-years which corresponds to ~ 12years of age at the time of 1987 image acquisition. The accuracy of the classified image was assessed by quantifying the proportion of “mature forest” category within individual age groups and the total forests greater than 12 years of age. The results of the assessment show that “mature tree” category consistently represents the majority of pixels within the validation polygons. On average 58% of pixels within the inventory polygons were classified as “mature forest” and 18% of pixels were not classified successfully within the 0.7 probability threshold. The lowest percentage of pixels classified as “mature forest” (39%) was found in the category of forests 7- 12 years old at the time of image acquisition which may not be representative of truly “mature” stands.

Tree age category	Number of pixels mapped					% pixels within the category				
	<i>unclass</i>	<i>bare</i>	<i>shrub</i>	<i>tree</i>	<i>tree.mort</i>	<i>unclass</i>	<i>bare</i>	<i>shrub</i>	<i>tree</i>	<i>tree.mort</i>
7 - 12years	1532	124	915	2713	1698	22%	2%	13%	39%	24%
12-17 years	1269	184	1916	9527	741	9%	1%	14%	70%	5%
17-22 years	12287	1465	12086	43760	4089	17%	2%	16%	59%	6%
22-27 years	3848	378	5643	28746	2160	9%	1%	14%	70%	5%
27-32 years	22902	2165	14082	69713	8192	20%	2%	12%	60%	7%
32-37 years	2484	220	4026	29863	1944	6%	1%	10%	77%	5%
37-42 years	28596	2962	23453	94243	14313	17%	2%	14%	58%	9%
42-47 years	679	23	2099	12074	128	5%	0%	14%	80%	1%
47-52 years	21623	1675	19782	87045	7075	16%	1%	14%	63%	5%
52-57 years	1091	155	781	4249	337	16%	2%	12%	64%	5%
> 57 years	94540	5392	69718	248309	58213	20%	1%	15%	52%	12%
Total	190851	14743	154501	630242	98890	18%	1%	14%	58%	9%

6.1.2.2 Scene from July 5, 2006

Development of validation data set for the accuracy assessment of the maximum likelihood classification based on the 2006 image was more difficult. Considering that the in situ inventory data were collected during 2000, information regarding the spatial extent of subsequent disturbances by fire (confirmed by the MODIS active fire detections) and logging (confirmed by visual interpretation of the image by the analyst) was not available. Visual analysis confirmed that the southern section of the image which included a large section of forest inventory data underwent a considerable amount of change (primarily from forest logging) since 2002.

Subsequently, the inventory set from the southern section was excluded from further analysis.

Class	# pixels	% pixels
<i>unclass</i>	162	0%
<i>bare</i>	8903	4%
<i>shrub</i>	61797	25%
<i>tree</i>	174619	71%
<i>tree.mort</i>	1243	1%

The northern section of the image containing inventory data was also modified by fire occurrence since 2000. The central section of the inventory data was least affected by disturbance since 2002. Tree dominated land cover classes of all stand ages from the central region inventory data were included in the “mature forest” class accuracy assessment. The results show that the “mature tree” category represents more than 70% of pixels within

the target classes.

6.2 Change detection

Change detection was based on the Disturbance Index (DI) methodology developed by Healy et al. (2005). The “mature forest” masks (section 6.1.1) were used to normalize the TC brightness, greenness, and wetness components to that of the mature forests following

$$B_r = (B - B_\mu) / B_\sigma$$

$$G_r = (G - G_\mu) / G_\sigma$$

$$W_r = (W - W_\mu) / W_\sigma$$

where B_r , G_r , W_r is rescaled Brightness, Greenness and Wetness, B_μ , G_μ , W_μ is mean Brightness, Greenness, and Wetness of “mature forest”, and B_σ , G_σ , W_σ is standard deviation of Brightness, Greenness, and Wetness in “mature forest”.

The DI is then calculated following

$$DI = B_r - (G_r + W_r)$$

The common extent of the three scenes was defined and tree cover change was assessed using the maximum likelihood classification of the multi-temporal DI stack (1987-2002-2006). The training data was selected by the analyst based on visually identifiable disturbance and regrowth patterns within the three scenes. Forest change was mapped only within areas identified as “tree dominated” during any of the mapping years, i.e. 1987, 2002 or 2006. Areas with other dominant land cover types were masked out.

The three-time-steps change detection methodology allowed for identification of the following 10 classes of change.

<i>Class</i>	<i>Class name</i>	<i>Description</i>
1	dist_87_02	disturbance occurred between 1987 and 2002 with slow subsequent regrowth by 2006
2	regr_87_02	regrowth between 1987 and 2002 with continuing regrowth by 2006
3	dist_02_06	disturbance occurred between 2002 and 2006
4	regr_02_06	regrowth between 2002 and 2006
5	UNF	undisturbed non-forest
6	UF	undisturbed forest
7	regr_02_dist_06	regrowth between 1987 with a subsequent disturbance by 2006
8	dist_02_regr_06	disturbance occurred between 1987 and 2002 with noticeable subsequent regrowth by 2006
9	dist_87_dis_02	burned areas in 1987 were reburned by 2002
10	fill	fill values including cloud cover, cloud shadows, and water

6.3 Post-classification processing

A 5-consecutive pixels minimum filter is run to eliminate potential noise of the resultant change. The eliminated pixels were filled using the iterative majority analysis within a 5X5 kernel. In cases where a 5X5 kernel was insufficient, the kernel size was increased sequentially to 7X7, 9X9, and 11X11.

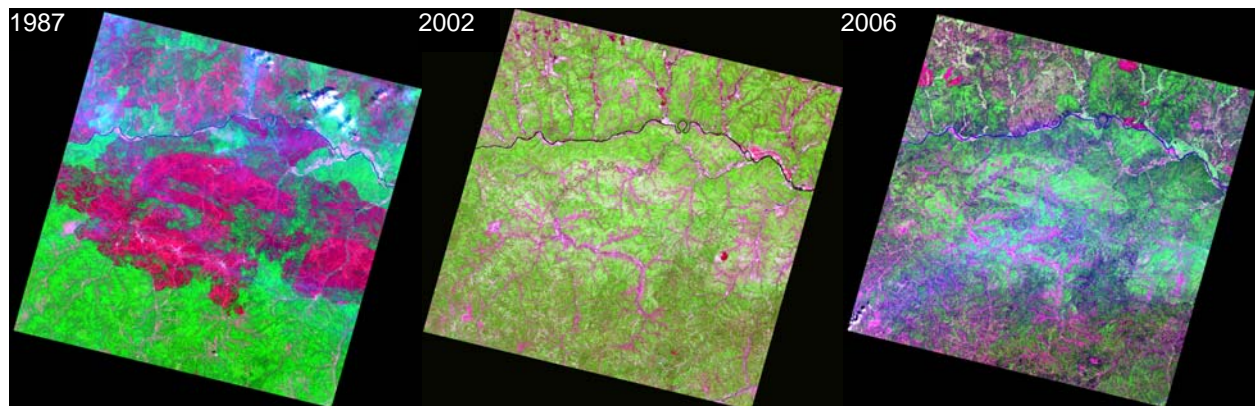
6.4 Accuracy assessment

The accuracy assessment approach follows the random pixel selection and analyst interpretation described in section 5.4. The distribution of accuracy assessment points was split by ~150 pixels for “unchanged” and ~150 pixels for “changed” classes. Within each of the classes, the number of validation pixels was assigned proportionally to the class size but no less than 30 pixels. Due to very low number of pixels in class 7 (0.2% see section 6.5) this class was omitted from accuracy assessment. Class “dist_87_dist_02” presents a single large burned area in 2002 within the extremely large burned area of 1987; therefore the class was also omitted from the accuracy assessment.

Predicted class	Observed class							Sum	Committed %
	D_87	R_87	D_02	R_02	UNF	UF	R_02		
	_02	_02	_06	_06			_D06		
dist_87_02	29	0	4	0	4	3	0	40	27.5
regr_87_02	0	50	1	0	0	3	1	55	9.09
dist_02_06	2	6	45	0	0	21	0	74	39.19
regr_02_06	1	2	0	23	0	6	3	35	34.29
UNF	13	0	3	0	26	7	0	49	46.94
UF	3	1	7	0	1	71	0	83	14.46
dist_02_regr_06	5	2	2	9	0	1	60	79	24.05
Sum	53	61	62	32	31	112	64	415	
Omission %	45.28	18.03	27.42	28.13	16.13	36.6	6.25		
Overall Accuracy = 73.25%									
Kappa Coefficient = 0.6827									

6.5 Results of the land cover change map

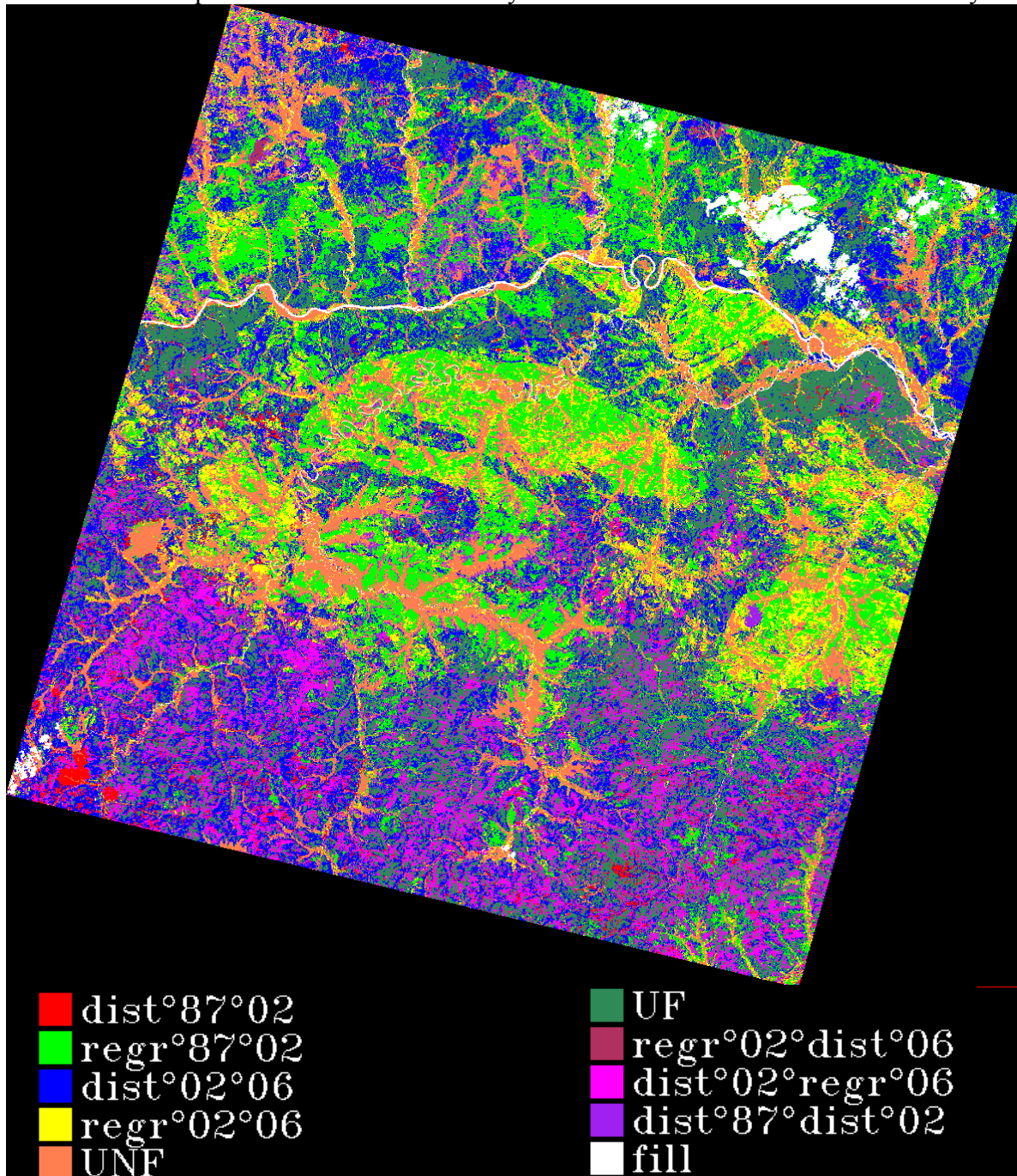
The forests of the selected study site were strongly altered within the time-frame of this analysis.



Class	Pixels	Area (ha)	% study area
dist_87_02	972925	87563.25	3%
regr_87_02	6255360	562982.4	18%
dist_02_06	7352558	661730.2	21%
regr_02_06	3504902	315441.2	10%
UNF	5145950	463135.5	14%
UF	7202690	648242.1	20%
regr_02_dist_06	80889	7280.01	0%
dist_02_regr_06	2769142	249222.8	8%
dist_87_dis_02	1471431	132428.8	4%
fill	779367	70143.03	2%

Visual analysis shows that wildland fire is a major disturbing agent in the forests in the Amur site. Fire scars are clearly discernable in the imagery for each of the analyzed years, however, the catastrophic fire of 1987 exceeds by far the impact from wildland fires on the forests since

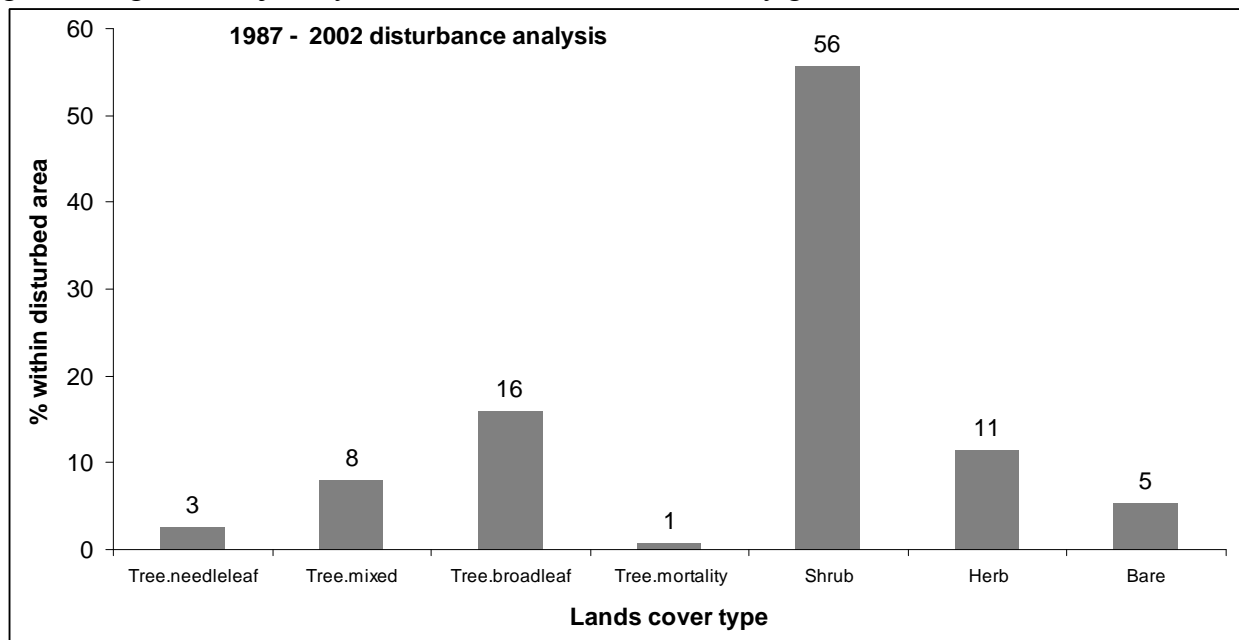
that year. Change detection analysis indicates that after this extreme fire event, only 3 percent of forest cover was changed to non-tree dominated land covers between 1987 and 2002. By 2002 most of area burned in 1987 returned to tree-dominated communities and accounted for 18% regrowth captured by the change detection mapping. A small (0.2%) portion of forests which regrew by 2002 was subsequently disturbed again by 2006. The majority of disturbance between 2002 and 2006 resulted from logging activities in the southern section of the study area which was previously not affected by 1987 fire. Approximately 10% of forest was gained between 2002 and 2006, however the large proportion of that number present a continuing regrowth of the forests disturbed prior to 1987 which had not yet formed tree-dominated communities by 2002.



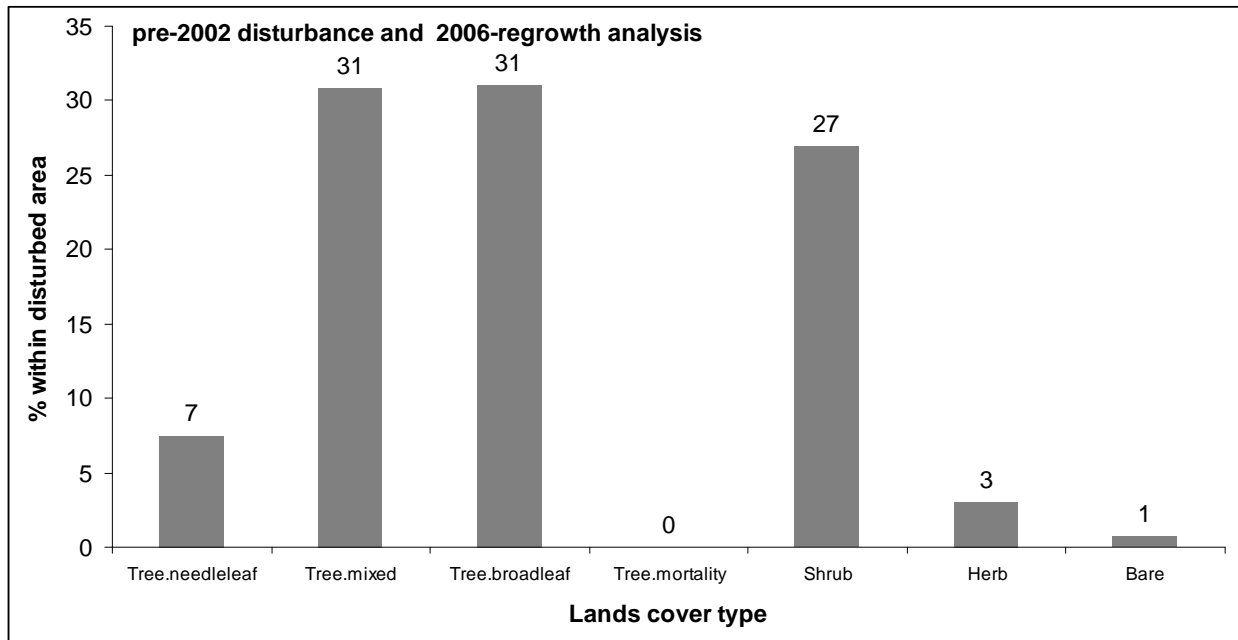
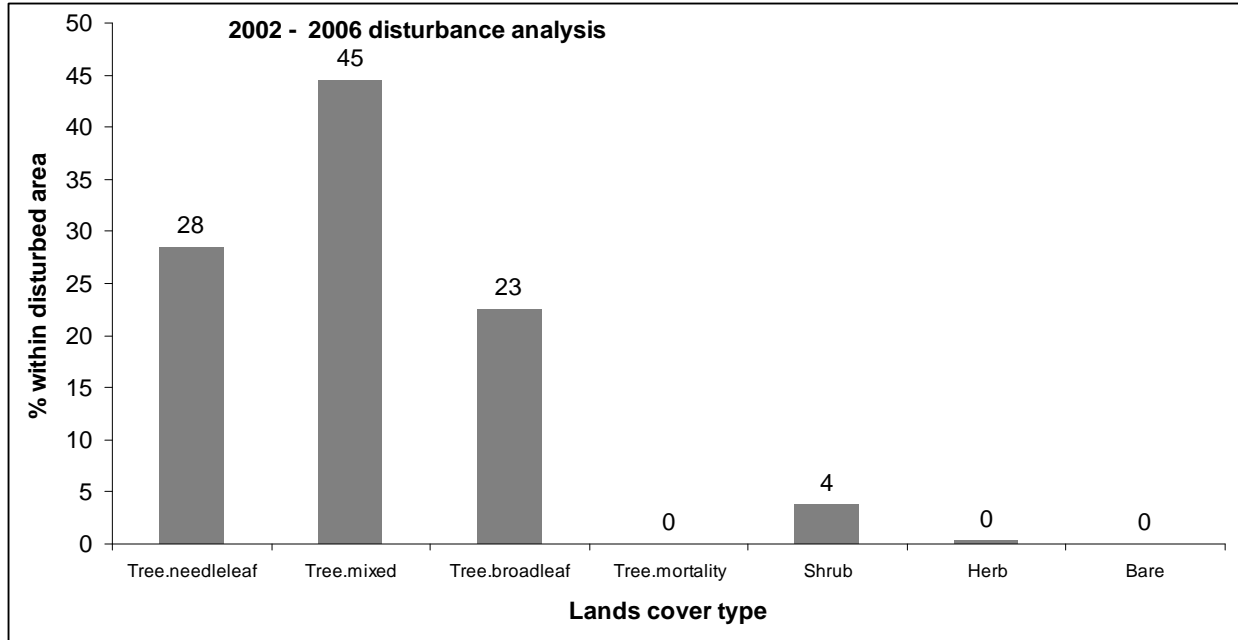
Overall, forests in the Amur site exhibit relatively fast regrowth. The 8% gain in tree-dominated landscapes by 2006 resulted from regrowth of sites disturbed between 1987 and 2002. Local experts advise that these rates of regrowth may reflect the reforestation strategies adopted by the Chinese forestry professionals and thus are not representative of natural regrowth rates. This suggestion is supported by the lack of regrowth in the northern section of the study site which is located within Russian Federation and thus is under a different forestry management approach.

6.6 Analysis of the land cover change map

The analysis of the 1987-2002 disturbed areas in comparison with land cover distribution mapped from 2002 image shows that nearly 56% of disturbed areas were in a “shrub-dominated” stage of the community regrowth and did not return to tree-dominated communities. Of those that returned to tree-dominated communities only 3% were predominantly needleleaf forests, 8% were mixed forests and 16% were in the broadleaf dominated communities consistent with the general regrowth trajectory for boreal forests with secondary growth succession.



The analysis of disturbances between 2002 and 2006 showed that 96% of affected areas were within tree dominated stands with ~28% within tree.needleleaf class, ~45% within tree.mixed class and ~23% within tree.broadleaf class. These findings are consistent with the results of visual analysis which show that the majority of post-2002 disturbance is represented by forest harvesting rather than wildland fire activity. Forest harvesting targets economically valuable needleleaf species rather than less valuable successional birch and aspen forests. The analysis of pre-2002 disturbances which demonstrated considerable amount of regrowth by 2006 shows a larger proportion of tree-dominated communities with robust presence of both broadleaf (31%) and mixed (31%) forests indicative of reforestation efforts and consistent with the results of visual analysis discussed in section 6.5.



7 Publications Using the Site Data

None.

8 List of Contributors to Site Data and Report

Tatiana V. Loboda

University of Maryland
Geography Department
2181 LeFrak Hall
College Park, MD 20742

Guoqing Sun

University of Maryland
Geography Department
2181 LeFrak Hall
College Park, MD 20742

Zhiyu Zhang

University of Maryland
Geography Department
2181 LeFrak Hall
College Park, MD 20742

9 Acknowledgements

This research was supported by the NASA Land Cover Land Use Change Program Grant # NS175AA.

10 References

- Chavez, P.S., Jr. (1996). Image-based atmospheric corrections: Revisited and improved. *Photogrammetric Engineering and Remote Sensing* **62**, 1025–1036.
- Crist, E.P. (1985). A TM Tasseled Cap Equivalent Transformation for Reflectance Factor Data. *Remote Sensing of Environment* **17**, 301-306.
- Healy, S.P., Cohen, W.B., Zhiqiang, Y., Krankina, O.N. (2005). Comparison of Tasseled Cap-based Landsat data structures for use in forest disturbance detection. *Remote Sensing of Environment* **97**, 301-310.
- Loboda, T., O’Neal, K.J., Csiszar, I. (2007). Regionally adaptable dNBR-based algorithm for burned area mapping from MODIS data. *Remote Sensing of Environment* **109**, 429-442.
- Soenen, S.A., Peddle, D.R., Coburn, C.A. (2005). SCS+C: A modified sun-canopy-sensor topographic correction in forested terrain. *IEEE Transactions on Geoscience and Remote Sensing* **43**(9), 2148-2159.
- Zhang, P., Shao, G., Zhao, G., Le Master, D.C., Parker, G.R., Dunning, J.B., Li, Q. (2000) China’s forest policy for the 21st century. *Science* (**288**), 2135-2136.
- Zhao, G., Shao, G.F. (2002) Logging restrictions in China – A turning point for forest sustainability. *Journal of Forestry* **100** (4), 34-37.